processes

MDPI

Article

Anandamide Reuptake Inhibitor (VDM11) as a Possible Candidate for COVID-19 Associated Depression; a Combination of Network Pharmacology, Molecular Docking and In Vivo Experimental Analysis

Sami I. Alzarea [1,*], Sumera Qasim [1,*], Muhammad Afzal [1], Omar Awad Alsaidan [2], Hassan H. Alhassan [3], Metab Alharbi [4], Mohammed Alqinyah [4] and Fahaad S. Alenazi [5,6]

[1] Department of Pharmacology, College of Pharmacy, Jouf University, Sakaka 72341, Saudi Arabia
[2] Department of Pharmaceutics, College of Pharmacy, Jouf University, Sakaka 72341, Saudi Arabia
[3] Department of Clinical Laboratories Sciences, College of Applied Medical Sciences, Jouf University, Sakaka 72341, Saudi Arabia
[4] Department of Pharmacology and Toxicology, College of Pharmacy, King Saud University, Riyadh 11451, Saudi Arabia
[5] Department of Pharmacology, College of Medicine at the University of Ha'il, Hail 55476, Saudi Arabia
[6] Medical Education Unit, College of Medicine at the University of Ha'il, Hail 55476, Saudi Arabia
* Correspondence: samisz@ju.edu.sa (S.I.A.); qsumera@ju.edu.sa (S.Q.)

Abstract: Objective: Post-COVID 19 depression has gained much attention due to the increasing percentage of depressive symptoms reported by COVID-19 survivors. Among many factors postulated to be responsible for this depression, neuroinflammation gained the most attention. Therefore, in current work, we selected an anandamide reuptake inhibitor, VDM11, as a possible candidate for managing post-COVID depression. Methods: The role of VDM11 in attenuating neuroinflammation was established by using network pharmacology, molecular docking, and an in vivo LPS-induced depression model. Results: The results of network pharmacology revealed that among all the genes that can be targeted by VDM11, 47 genes were directly linked to the pathophysiology of depression. Additionally, on the basis of protein–protein interaction (PPI) analysis, the top 10 hub genes probably responsible for VDM11 antidepressant attribute were screened. These genes include MAPK3, TNF-α, IL-1β, IL-6, PPARG, MAPK1, CNR1, MTOR, NR3C1, and IGF1R. These genes were also enriched in GO and KEGG analysis. Molecular docking was carried out with top five hub genes screened by PPI network and KEGG analysis which showed that VDM11 interacts well with these targets. The antidepressant potential of VDM11 was also assessed by employing a LPS-induced depression model. Animals provided with VDM11 demonstrated increased exploration time and spontaneous alterations in elevated plus and Y maze models. Additionally, the level of astrocyte marker GFAP, microglia marker CD11b, and proinflammatory cytokines, including TNFα, IL-1β, and IL-6, in the hippocampus were significantly reduced by VDM11, further strengthening its role in neuroinflammation. Conclusion: VDM11, an anandamide reuptake inhibitor, might serve as a possible candidate for post-COVID depression, probably by modulating neuroinflammation. However, detailed pharmacological studies are required to validate these outcomes.

Keywords: anandamide reuptake inhibitor; VDM11; network pharmacology; molecular docking; LPS-induced depression; post-COVID depression

check for updates

Citation: Alzarea, S.I.; Qasim, S.; Afzal, M.; Alsaidan, O.A.; Alhassan, H.H.; Alharbi, M.; Alqinyah, M.; Alenazi, F.S. Anandamide Reuptake Inhibitor (VDM11) as a Possible Candidate for COVID-19 Associated Depression; a Combination of Network Pharmacology, Molecular Docking and In Vivo Experimental Analysis. *Processes* **2023**, *11*, 143. https://doi.org/10.3390/pr11010143

Academic Editors: Alina Pyka-Pajak and Mahesh Narayan

Received: 4 December 2022
Revised: 21 December 2022
Accepted: 28 December 2022
Published: 3 January 2023

Copyright: © 2023 by the authors. Licensee MDPI, Basel, Switzerland. This article is an open access article distributed under the terms and conditions of the Creative Commons Attribution (CC BY) license (https://creativecommons.org/licenses/by/4.0/).

1. Introduction

The SARS-CoV-2 (Severe Acute Respiratory Syndrome Coronavirus 2) pandemic, which started in China in December 2019, is still spreading around the globe. The World Health Organization (WHO) estimates that the coronavirus disease 2019 (COVID-19) pandemic has killed more than 6 million people and infected about 500 million people world-

wide. Since the pandemic's onset, there have been reports of psychopathological effects during acute infection and in the post-COVID-19 phase in COVID-19 survivors. After acute viral infection, symptoms such as confusion, delirium, sadness, anxiety, and sleep problems have been observed [1]. At 1-, 3-, 6-, and 12-month follow-up subsequent to SARS-CoV-2 infection, approximately 30–40% of patients had clinically severe depressive psychopathology. Depression, which is characterized by low mood, loss of interest, and cognitive decline, has a negative impact on day-to-day activities. A greater infection risk, hospitalization, admission to an intensive care unit, and mortality were observed to be associated with both pre-existing depression and COVID-19-related depressive symptoms [2]. The immunological inflammatory response to the viral infection, as well as the psychological stressors due to SARS-CoV-2 infection, were postulated to be the key factors contributing to the COVID-19 mental sequelae [3]. Therefore, it is important to identify, classify, and manage post-COVID depression symptoms.

The CNS is among the expanding number of biological systems whose physiological functions might be affected by the SARS-CoV-2 infection. Post COVID-19, CNS neuropathological alterations have been observed in many patients [4]. Pro-inflammatory mediators are released as a result of these alterations, resulting in unnecessary inflammatory responses. Recent clinical investigations have demonstrated that inflammation was induced in COVID-19 patients, and this induction was linked to an upregulation in cytokines such as tumor necrosis factor (TNF-α), interleukin (IL)-1, IL-6, and IL-10 [5]. According to previous studies, cytokines-induced tight junction (TJ) protein degradation promotes inflammation, thus altering blood–brain barrier (BBB) integrity. TJ deterioration increases BBB permeability [6]. When the BBB's integrity is compromised, viruses and cytokines have a greater chance of penetrating the central nervous system (CNS) with resultant activation of cerebral immune cells (astrocytes and microglia) and, ultimately, neuroinflammation. An analysis of a postmortem study of 43 COVID-19 patients revealed that 37 of them had astrogliosis, 34 had microglial activation in the brainstem and cerebellum, and 6 had ischemic lesions [7]. Microglial cells are more vulnerable to infections than astrocytes, and it has been found that systemic infection can provoke their activation in the CNS. Activated microglia leads to the production of IL-1 and TNF, which in turn stimulates astrocytes activation. Activated astrocytes can produce a variety of inflammatory mediators, such as TNF-α, ROS, and nitric oxide (NO). Thus, the cascaded neuroinflammation is exacerbated by the interaction between astrocytes and microglia [8].

A biological modulatory system called the endocannabinoid system (ECS) is present in the central nervous system (CNS) and peripheral tissues of the majority of vertebrates. This system comprised two primary endocannabinoid receptors (CB1 and CB2), their endogenous ligands, endocannabinoids (anandamide and 2-arachidonoyl glycerol), and a variety of specialized enzymes for the production and degradation of endocannabinoids [9]. For the homeostatic maintenance of physiological, cognitive, behavioral, and emotional processes, there should be an appropriate interaction between all the components of the ECS. Deficits in cognition may therefore appear when the ECS is dysregulated [10]. A symptomatic overlap has been manifested by various animal studies among depressive disorder and ECS alterations. Endocannabinoids have variable affinities for binding to CB1 and CB2 receptors in the presynaptic membrane after release [11]. Anhedonia, passive stress-coping, and an increased susceptibility to developing depressive symptoms are all caused by CB1 ablation. A possible antidepressant effect could result from the administration of a CB1 agonist or from higher endocannabinoid levels [12].

VDM11 is a selective anandamide reuptake inhibitor which elevates the anandamide level by inhibiting fatty acid amide hydrolase (FAAH) [13]. Elevation in the anandamide level has been postulated to be a useful strategy for combating depressive disorder. In the current investigation, an attempt was made to explore the possible role of VDM11 in managing depression, especially focusing on post-COVID depression as an ongoing issue. To validate the role of VDM11, a combination of network pharmacology, molecular

docking, and in vivo experiments were conducted to elucidate a possible antidepressant mechanism of VDM11.

2. Material and Methods

2.1. Network Pharmacology

2.1.1. Screening of Target Genes for VDM11 and Disease-Associated Genes

Target genes for VDM11 were predicted using Swiss target prediction (http://www.swisstargetprediction.ch/) and the Binding DB (https://www.bindingdb.org/rwd/bind/index.jsp), accessed on 10 August 2022 [14].

2.1.2. Protein–Protein Interaction Network Construction and Analysis

The online database STRING 11.0 may gather, evaluate, and integrate knowledge about protein–protein interactions from all publicly accessible sources (https://string-db.org/, accessed on 3 December 2022). The species was set to Homo sapiens, and a minimum interaction score of 0.7 was used to generate a protein interaction network. The information was inserted into Cytoscape 3.9.1 for visual analysis [15].

2.1.3. Target Protein Gene Ontology and KEGG Enrichment Analysis

Target genes screened for the VDM11 antidepressant mechanism were screened for their role in gene function and signaling pathways by using the database for annotation, visualization, and integrated discovery (David) v 6.8 [16]. Cellular components (CC), molecular functions, biological processes, and pathways were all screened for target genes. KEGG pathway bubble charts made with SRPLOT (http://bioinformatics.com.cn/, accessed on 3 December 2022) were of particular interest [17].

2.2. Molecular Docking

MOE 2015 was used as the molecular docking tool for ligand docking studies into the binding pocket of the top five target proteins identified via PPI networking. The protein data bank contained the crystal structures of the target proteins (MAPK3, TNF, IL1B, IL6, and PPARG) (PDB IDs: 4QTB, 2AZ5, 1ITB, 1ALU, and 2PRG). The 3D structures of these targets with mentioned PDB ID were retrieved from the protein data bank. The structure of VDM11 and positive controls were prepared using the MOE builder tool. Using the energy-minimization method of the MOE tool, the energy of the protein molecule was reduced. To reduce energy, variables such as the 0.05 Gradient, MMFF94X + Solvation Force Field, and Current Geometry Chiral Constraint were used. When the root mean square gradient fell to less than 0.05, energy minimization was stopped [18]. The site finder tool of MOE was employed to determine the binding pocket of target proteins. Ten distinct docked conformations were produced after the active site was chosen. Binding pattern analysis was performed using the compound's lowest energy conformation [14].

Molecular docking studies were also performed for positive controls, including minocycline [19], thalidomide [19], PKF115-584 [20], bazedoxifene [21], and thiazolidinedione [22].

2.3. Experimental Pharmacology

2.3.1. Experimental Animals

Healthy male Wistar albino mice of optimum weight (20–25 g) were selected and habituated to laboratory conditions for 7 days in ambient surroundings of an animal housing facility, comprising a 12:12 h (light and dark) cycle, 23 ± 2 °C temperature, and 55% humidity on average, with free access to normal rodent chow diet and water ad libitum. Local Committee of Bioethics at Jouf University, Sakaka, Aljouf, Saudi Arabia (6-02-42) approved the Experimental protocol. All the experimental procedures were carried out at the Pharmacology laboratory of College of Pharmacy, Jouf University, Sakaka, Al-Jouf, Saudi Arabia.

2.3.2. Chemicals

AM251, AM630, VDM11, and LPS (*Escherichia coli*, serotype 0127:B8) were all procured from TRC Inc., 20 MARTIN Ross Avenue, North York, Canada.

2.3.3. Study Design

The experimental protocol was divided into two sections: section A and section B.

Section A was further divided into two steps comprising of 8 groups of Wistar albino mice (n = 6). Four groups of animals were designated as drug-treatment groups. Group I served as vehicle + saline treated, group II animals were administered with normal saline and VDM11 1 mg/kg, and group III animals administered with saline and VDM11 4 mg/kg. Similarly, group IV animals were fed with saline and VDM11 10 mg/kg.

Another 4 groups of animals were the treatment controls. Among them, Group 1 served as LPS control and was administered with LPS (0.5 mg/kg)+ Vehicle. Group II, III, and IV animals were administered with VDM11 (1, 4, 10 mg/kg), respectively, and 30 min later, LPS (0.5 mg/kg) IP was injected into each.

Section B of the experiment was conducted to study and confirm the role of anandamide reuptake inhibitor in depression. Step 1 comprised 4 groups designated as drug control groups. Group 1 was administered with Vehicle and saline only. Group II animals' scheduled treatment was AM251 (1 mg/kg) + AM630 (1 mg/kg) + Saline; Group III animals were administered with VDM11 (10 mg/kg) + saline, while the Group IV animals were administered with AM251 (1 mg/kg)+ AM630 (1 mg/kg) +VDM11 (10 mg/kg) + saline.

Step II experimental groups were split into 4 once again. Group 1 animals were administered with vehicle and LPS, Group II animals were administered with AM251 + AM 630 + LPS, Group III animals treatment scheduled as (VDM 11 + LPS), and Group IV animals were treated with AM251 (1 mg/kg) + AM630 (1 mg/kg) + VDM11 (10 mg/kg) + LPS (0.5 mg/kg) (Figure 1).

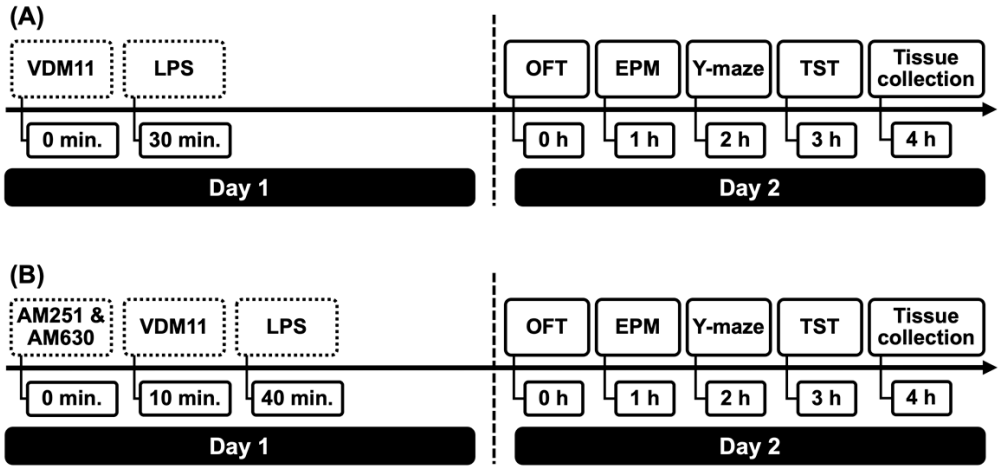

Figure 1. (**A**) Mice received different doses of VDM11 followed with LPS. (**B**) Mice received AM251 and AM630 together followed with effective dose of VDM11 and then LPS. Behavioral tests were carried out for both experiments. By the end of experiments, mice were sacrificed, and their brains were collected.

2.3.4. Open-Field Test (OFT)

To confirm the depression in animals after LPS exposure, an open field test (OFT) [23] was performed. Before conducting the test, animals were acclimated in the test room environment before an hour. To perform the test, a square box made up of plexiglass (50 cm × 50 cm × 40 cm) was used. There were 25 equal divisions in floor (10 cm × 10 cm) with noticeable lines. One mouse was placed in each box (10 cm × 10 cm) and allowed to walk around independently for 6 min. The total number of squares totally crossed by all four of its paws was taken into account and recorded as the locomotion. In order to

prevent any interference from animal urine and feces used in earlier tests, the equipment was cleaned following the test [24].

2.3.5. Elevated plus Maze (EPM) Test

Anxious behavior in rodents can be evaluated by EPM test. EPM apparatus is a "+"-shaped maze consisting of two open arms without walls (50 × 30 cm) and two closed (30 cm high walls) arms elevated above the floor. As rodents freely move through the maze, their behavior is recorded via a video recording device mounted above the apparatus and finally, a video tracking system is used to analyze the recordings. The preference to explore open arms over closed ones (expressed as % of time of open arms exploration) was calculated [25].

2.3.6. Y Maze Test

The exploratory activity was further tested using a Y-maze. The Y maze apparatus consisted of arms 40 cm in length, 3 cm bottom width, 13 cm arm width from the upper side, and a wall measuring 15 cm in height (Brain Science Idea, Osaka, Japan). To measure the exploratory behavior, each mouse was transferred gently and placed in the central area of the maze. The time spent exploring the arms was recorded for 10 min with a video-imaging system [26].

2.3.7. Tail Suspension Test

Tail suspension boxes with specific dimensions of (55 height × 60 width × 11.5 cm depth) were used. Each mouse was kept in its own rectangular, three-walled enclosure to prevent animals from looking at or interacting with one another. The mouse was suspended and the width and depth were satisfactorily gauzed to avoid the animals coming into contact with the walls. The mice were suspended above 20–25 cm from the nose (distance from the nose to floor).

2.3.8. Real-Time PCR Analysis

After conducting all tests described above, the brain was dissected from all animals. The prefrontal cortex was promptly separated from these samples and preserved at 80 °C for future use. The separated tissues were dealt with using the TRIzol® technique for total RNA extraction. To create cDNA from isolated RNA aliquots, Applied Biosystems' cDNA Reverse Transcription (high-Capacity) Kit and Master Cycler Personal were used. A quantitative polymerase chain reaction (qPCR) was carried out on the StepOnePlus quantitative real-time PCR equipment to determine the mRNA levels (Applied Biosystems). The assay utilized particular primers and the SYBR green PCR kit from Applied Biosystems (Integrated DNA Technologies, Coralville, IA, USA). The ΔΔCq method applied comparative GAPDH (housekeeping gene) to quantify the target gene's expression.

3. Results

3.1. Network Pharmacology Analysis

Using Binding DB and Swiss target prediction, 110 genes were associated with VDM11 (Supplementary Table S1), while DisGeNET-based depression genes prediction revealed 1478 genes. By comparing compound-related genes with depression-related genes, 47 overlapping genes were screened, which can be postulated to be the possible genes responsible for the antidepressant activity of VDM11 (Figure 2). Names of overlapping genes, along with their possible function, are mentioned in Supplementary Table S1. Details about all these genes were retrieved from the Gene cards Database (https://www.genecards.org/ (accessed on 3 December 2022)).

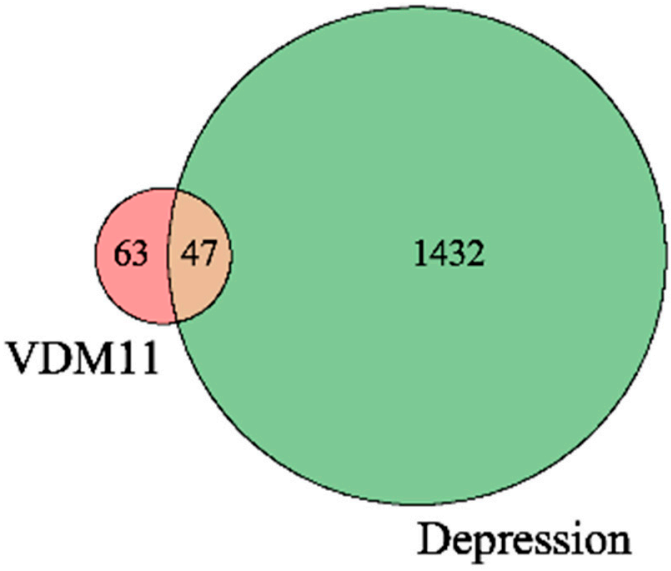

Figure 2. Overlapping genes between VDM11 and depression. The green color circle represents depression associated genes, pink color represents VDM11 targeted genes while brown color represents overlapping/common genes between VDM11 and depression.

The overlapped proteins were uploaded to STRING version 11.5, and high-certainty interacting proteins data with a score >0.7 were accepted for the PPI network development (Figure 3). The stronger the association between the proteins corresponding to the node in the network, the higher the degree in the network interaction, indicating that the target proteins play a vital part and are deemed to be the hub genes. Based on degree values, the ten topmost hub genes were screened, including MAPK3 (22), TNF (20), IL1B (19), IL6 (19), PPARG (18), MAPK1 (17), CNR1 (13), MTOR (13), NR3C1 (11), and IGF1R (10).

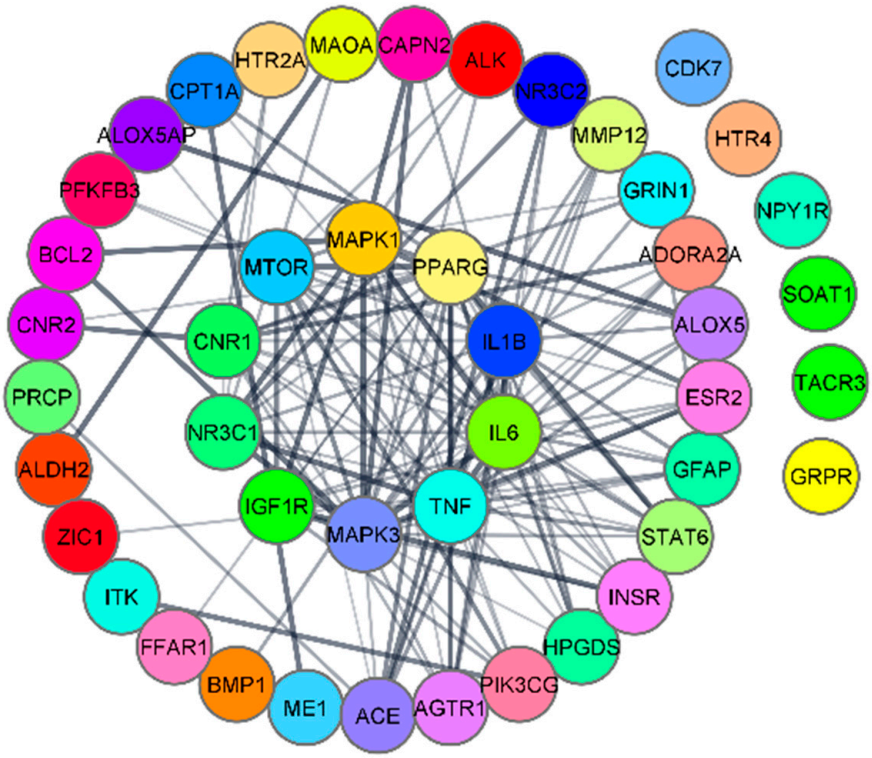

Figure 3. PPI network showing interaction among overlapping genes. The central nodes represent top ten interacting genes.

The functional annotation and enrichment analysis revealed potential biological functions of VDM11. According to GO functional analysis, VDM11 targets were related to regulation of acute inflammatory response, neuropeptide receptor activity, regulation of reactive oxygen species' metabolic processes, and so forth (Figure 4). The KEGG pathway analysis was performed to identify the significant signaling pathways' linked to VDM11 neuroinflammatory potential. It is noteworthy that most of the genes were involved in the following pathways: neuroactive ligand–receptor interactions (11), HIF-1 signaling pathway (8), AGE-RAGE signaling pathway (7), and Serotonergic synapse (5) (Figure 5). Finally, KEGG pathway analysis revealed that MAPK3, TNF, IL6, and IL1B were significantly enriched genes, as they contribute in multiple pathways associated with target genes.

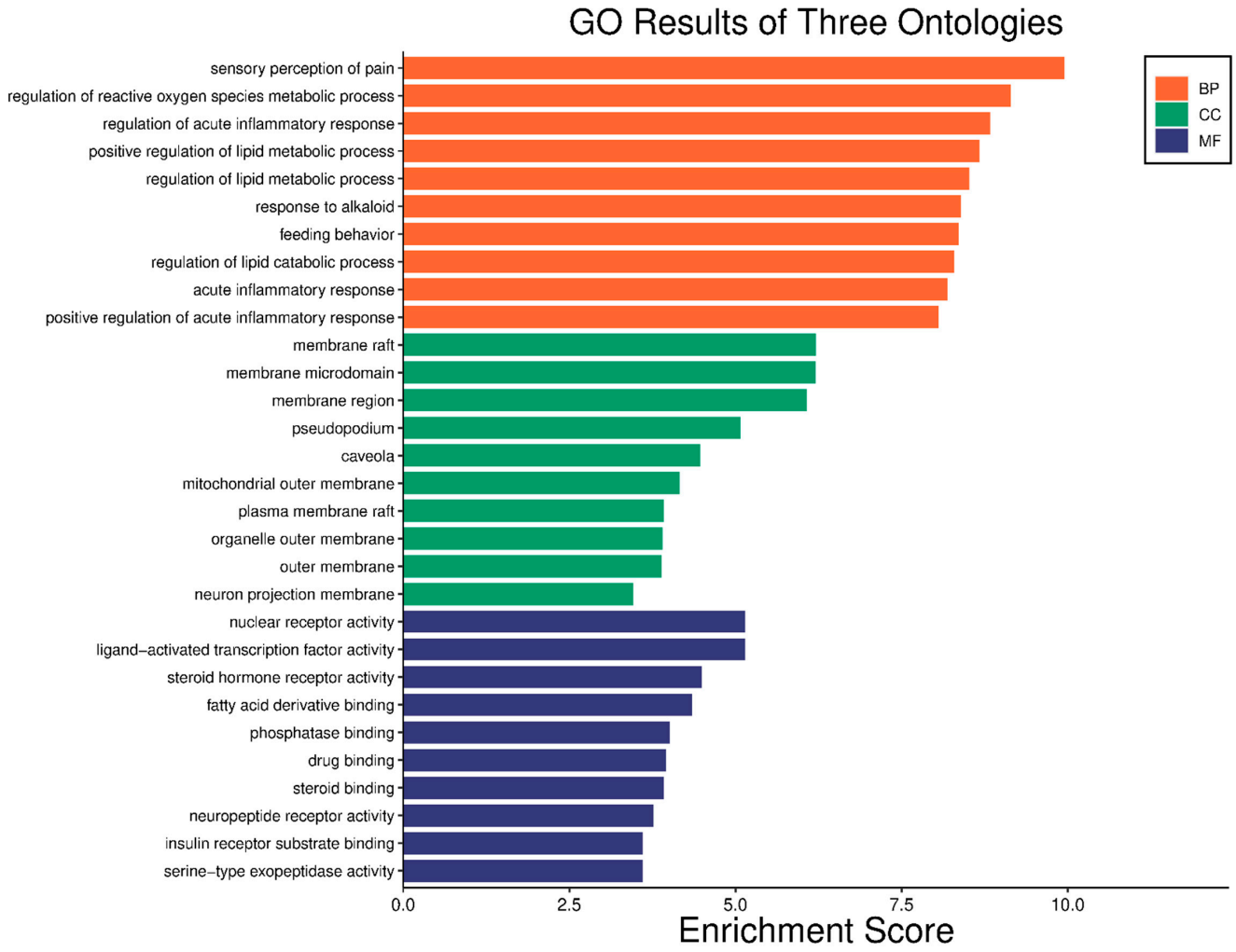

Figure 4. GO analysis in terms of biological process BP (orange color), cellular compartment CC (green color), and molecular function MF (blue color).

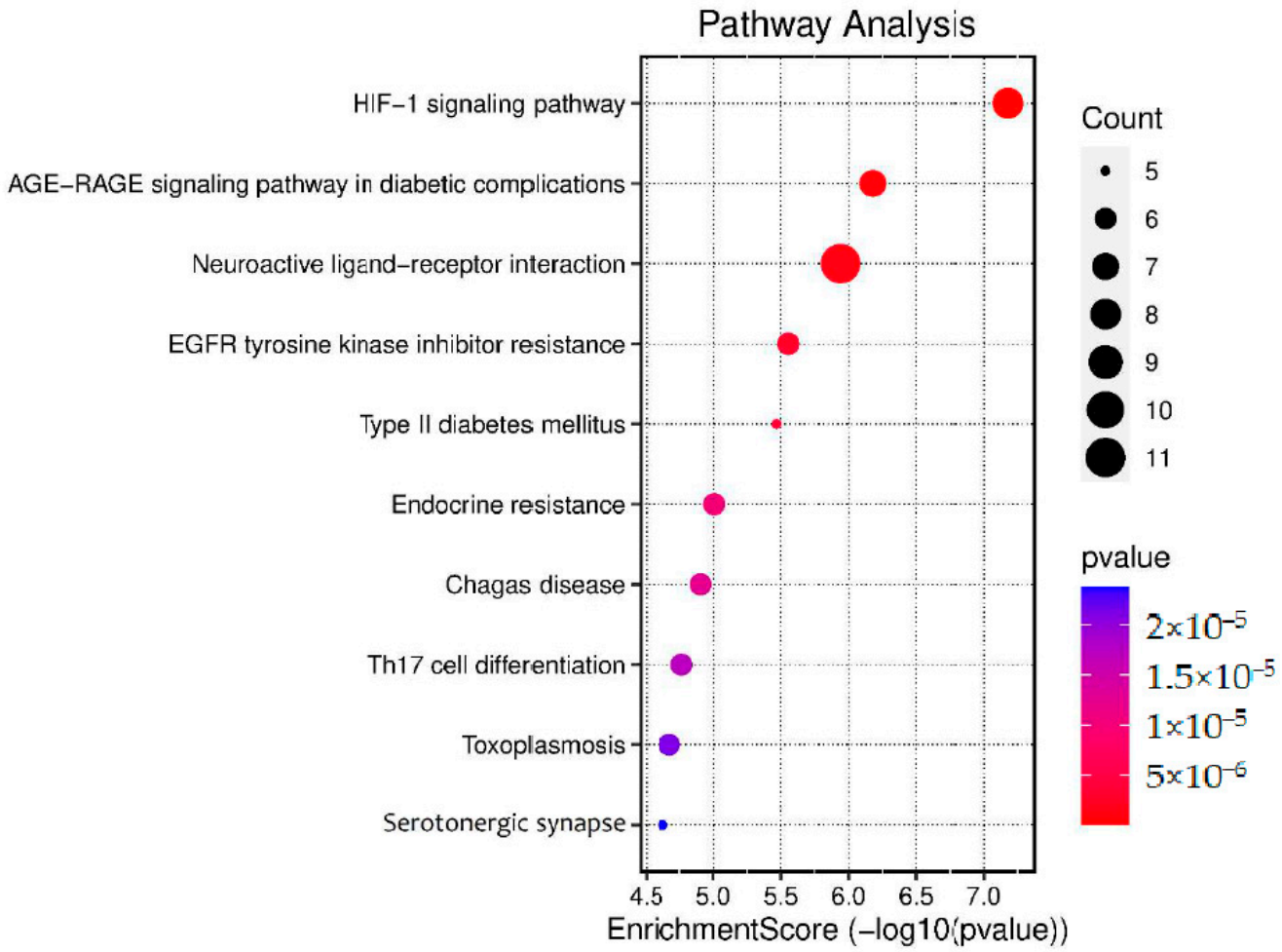

Figure 5. KEGG pathway analysis.

3.2. Molecular Docking

Docking of VDM11 with selected target genes (MAPK3, TNF, IL1B, IL6, and PPARG) revealed that all the compounds displayed strong binding affinity for selected target proteins and occupy the same site occupied by the co-crystallized ligand, as shown in Supplementary Figure S1a,b. The ligand–receptor combination is thought to interact strongly with the receptor when the binding energy is low. As a preliminary step for screening, active compounds exhibiting a binding energy ≥ -5.0 kcal/mol were chosen. Interestingly, a docking score of less than −5 kcal/mol was found for all target-VDM11 complexes, as shown in Table 1. Clusters with maximum binding energy and interaction were selected for final analysis.

Table 1. Binding mode analysis of VDM11 with selected targets.

Ligand–Receptor Complex	Docking Score (S) (kcal/mol)	Interaction			
		H-Bonding			Arene-π
		Residue	Distance (°A)	Score (%)	
VDM11-MAPK3	−10.6867	Lys168	2.36	98	
		Asp 166	3.16	70	
VDM11-TNF	−10.5469	SerB147	2.21	28	
VDM11-IL1B	−10.5514	SerA21	2.69	58	
		LysA27	2.71	44	
VDM11-IL6	−9.7890	Ser176	2.86	20	
		Arg179	2.85	61	
VDM11-PPARG	−9.9316	Arg288	2.71	11	Arg288

Moreover, minocycline, thalidomide, PK115-584, bazedoxifene, and thiazolidinedione were identified as positive control drugs of MAPK3, TNF, IL6 and PPARG, respectively. Comparison of binding energies and interaction of VDM11 with positive controls demonstrated that VDM11 displayed the highest binding energy, as well as strong interaction with TNF (2AZ5), as shown in Table 2.

Table 2. Binding mode analysis of positive controls with selected target proteins.

Control Drug	Target Protein	Docking Score (kcal/mol)	Interaction			
			H-Bonding			Arene-π
			Residue	Distance (°A)	Score (%)	
Minocycline	MAPK3	−12.6871	Lys53	2.91	17	
			Glu71	1.34	31	
			Asp 168	2.59	44	
Thalidomide	TNF	−7.4292	Asp168	1.99	20	
			AsnB34	2.63	23	ArgB32
PKF115-584	IL1B	−10.2315	SerA125	2.66	85	
Bazedoxifene	IL6	−11.5440	Arg30	2.73	63	Arg179
			Ser176	2.43	97	
Thiazolidinedione	PPARG	−10.5648	Ser342	2.46	95	

3.3. Experimental Pharmacology

3.3.1. Effect of VDM11 on LPS-Induced Depression in Mice Assessed through an Open Field Test (OFT)

After administration of vehicle and saline only and VDM 11 at 1, 4, and 10 mg/kg, respectively, along with saline, to experimental animals, OFT results reveal no significant differences in the number of crossings, which clearly depicts that there is no sickness behavior in the animals after 24 h. (Figure 6A). Similarly, exposure to LPS (0.5 mg/kg) after 30 min with the same treatment protocol of VDM 11 as of drug control groups (1, 4, 10 mg/kg), revealed no significant differences in the number of crossings observed. The effect of 10 mg/kg VDM 11 was greater, but insignificant (Figure 6A). Further, the number of crossings in the open field test (OFT) did not change significantly when mice received combination treatment of 1 mg/kg of AM251 (CB1 receptor antagonist) and 1 mg/kg AM630 (CB2 receptor antagonist) with 10 mg/kg of VDM1124 h after LPS administration (Figure 6B).

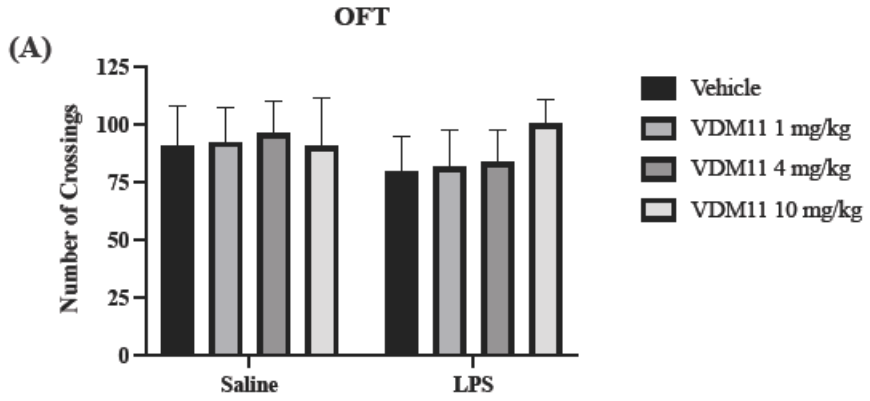

Figure 6. *Cont.*

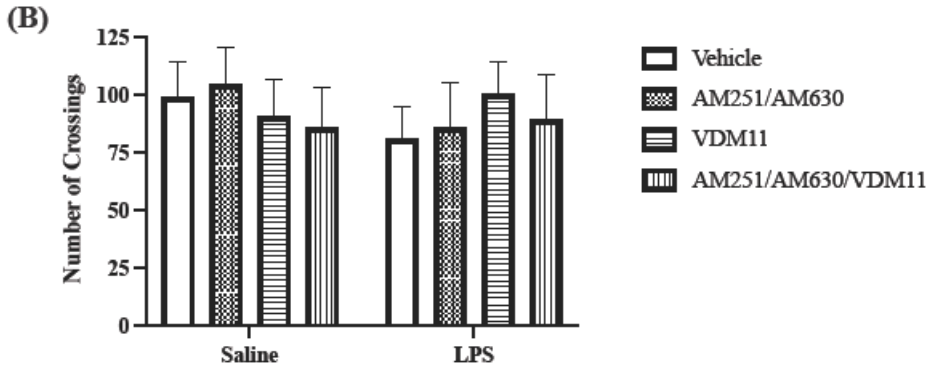

Figure 6. (**A**) Mice given various doses of VDM11, an anandamide reuptake inhibitor, 24 h after LPS injection did not significantly modify the number of crossings in the open field test (OFT). (**B**) Mice treated with a combination of 1 mg/kg each of the CB1 receptor antagonist AM251 and the CB2 receptor antagonist AM630, along with 10 mg/kg each of the anandamide reuptake inhibitor VDM11 24 h after LPS administration, did not experience a significant change in the number of crossings in the open field test (OFT).

3.3.2. Effect of VDM11on LPS-Induced Depression in Mice Assessed through Elevated plus Maze Test

The elevated plus maze test was performed after 25 h of LPS administration to experimental animals. The results of the test revealed that there were no significant differences in open arm exploration times in animals when treated with VDM 11 only at different doses. Meanwhile, administration of LPS to experimental animals significantly reduced the open arm exploration times % in animals. The open arm exploration time's percentage was found to be increased in animals which were pretreated with VDM11 at different dose levels. The most significant results were observed at 10 mg/kg of VDM11 pretreatment (Figure 7A). Combination treatment of CB1 and CB2 receptor antagonists (AM 251 and AM 630, respectively, 1 mg/ kg each) decreased open arm exploration times (%) in animals exposed to LPS, even in those pretreated with VDM11 at 10 mg/kg (Figure 7B).

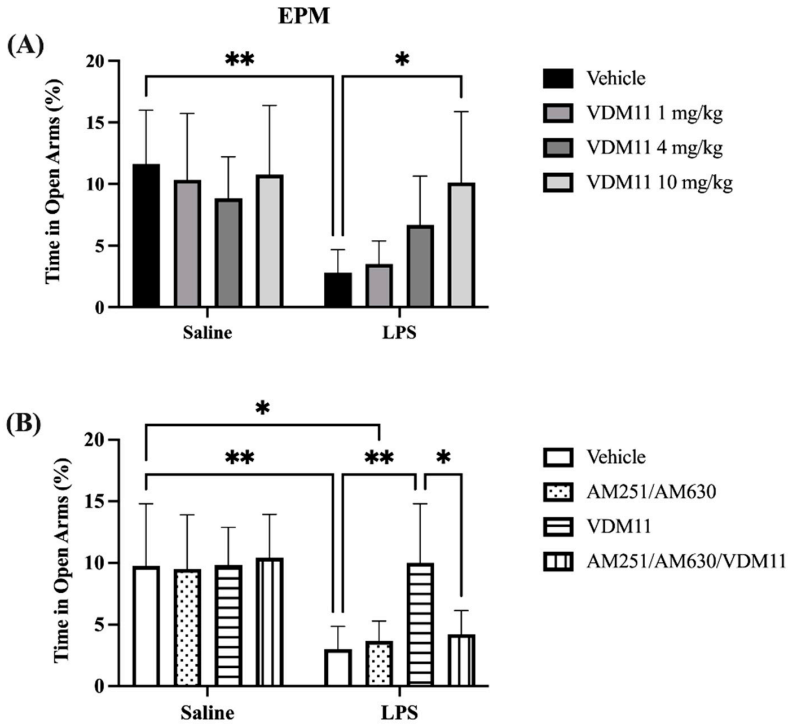

Figure 7. (**A**) VDM11 (anandamide reuptake inhibitor; 10 mg/kg) markedly enhanced exploration time in open arm (%) 25 h after LPS treatment. (**B**) Reduced effect of VDM11 on exploration time (%)

due to administration of CB1 receptor antagonist AM251 and the CB2 receptor antagonist AM630. * $p < 0.05$; ** $p < 0.01$.

3.3.3. Effect of VDM11on LPS-Induced Depression in Mice Assessed through Y Maze Test

The Y maze test was conducted after 26 h of LPS exposure in experimental animals. The results of the experiments performed exhibited that there were no significant differences observed in spontaneous alterations (%) in animals which were administered with normal saline + vehicle and different doses of VDM 11 alone. Exposing experimental animals to LPS significantly reduced spontaneous alterations (%), while the animals pretreated with VDM 11 at different doses and then exposed to LPS exhibited significantly elevated spontaneous alterations (%). The most significant results were recorded at 10 mg/kg of VDM11 (Figure 8A). Antagonism of CB1 and CB2 receptors (by AM251 and AM 630, respectively, in combination and alone) + reuptake inhibition of anandamide by VDM 11 (10 mg/kg) and then exposure to LPS revealed that combination treatment with AM251 and AM630 significantly reduced spontaneous alterations (%) activities in experimental animals, even after 10 mg/kg of VDM11 (Figure 8B).

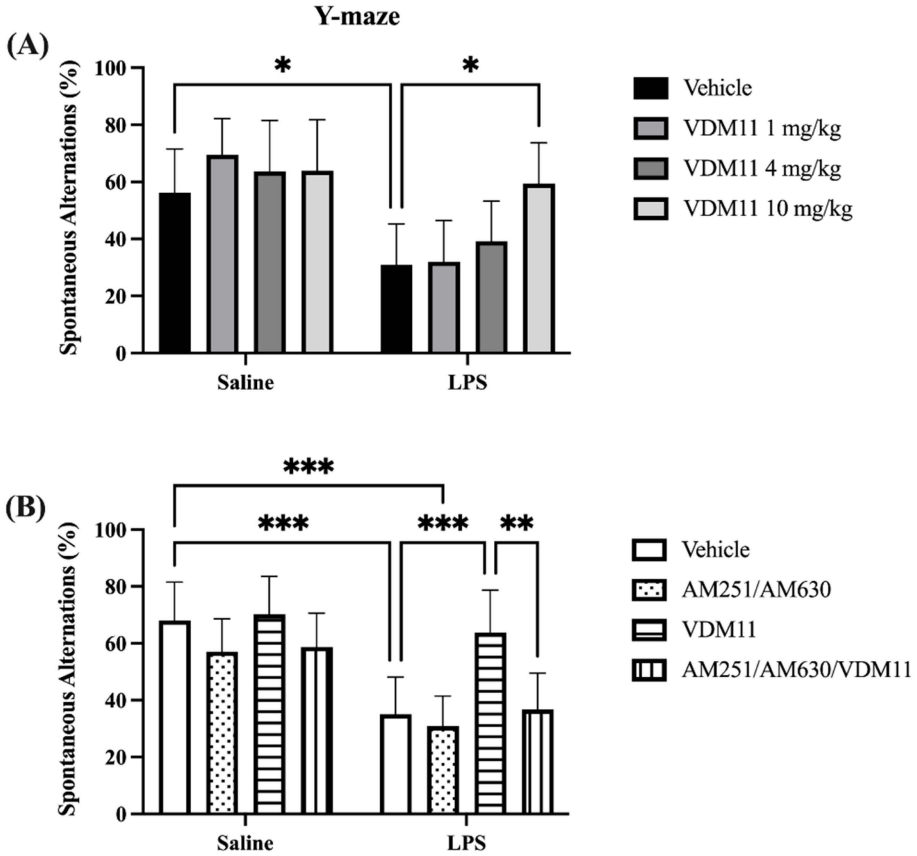

Figure 8. (**A**) In the Y-maze test performed on mice 26 h after LPS administration, VDM11 (an anandamide reuptake inhibitor; 10 mg/kg) significantly increased spontaneous alterations (%). (**B**) A combination treatment of 1 mg/kg each of the CB1 receptor antagonist AM251 and the CB2 receptor antagonist AM630 blocked the effects of 10 mg/kg of VDM11 on the percentage of spontaneous alternations that occurred during the Y-maze test 26 h after LPS administration in mice. * $p < 0.05$; ** $p < 0.01$; *** $p < 0.001$.

3.3.4. Effect of VDM11 on LPS-Induced Depression in Mice Assessed through Tail Suspension Test

Findings of the experiment performed after 27 h of LPS administration suggested that there were no significant alterations in immobility times in normal drug control animals which were treated with vehicle + saline and saline + VDM11 at different doses. Meanwhile, exposure of LPS to normal (vehicle-only treated) animals significantly increased the immobility times, which were observed to be near normal levels in animals pretreated with VDM11 at different doses before LPS administration. The most significant action was noticed at VDM11 10 mg/kg (Figure 9A). Antagonism of CB1 and CB2 receptors by administration of AM251 and AM630, respectively, attenuated the preventive effects of VDM 11 10 mg/kg on immobility times of the animals exposed to LPS (Figure 9B).

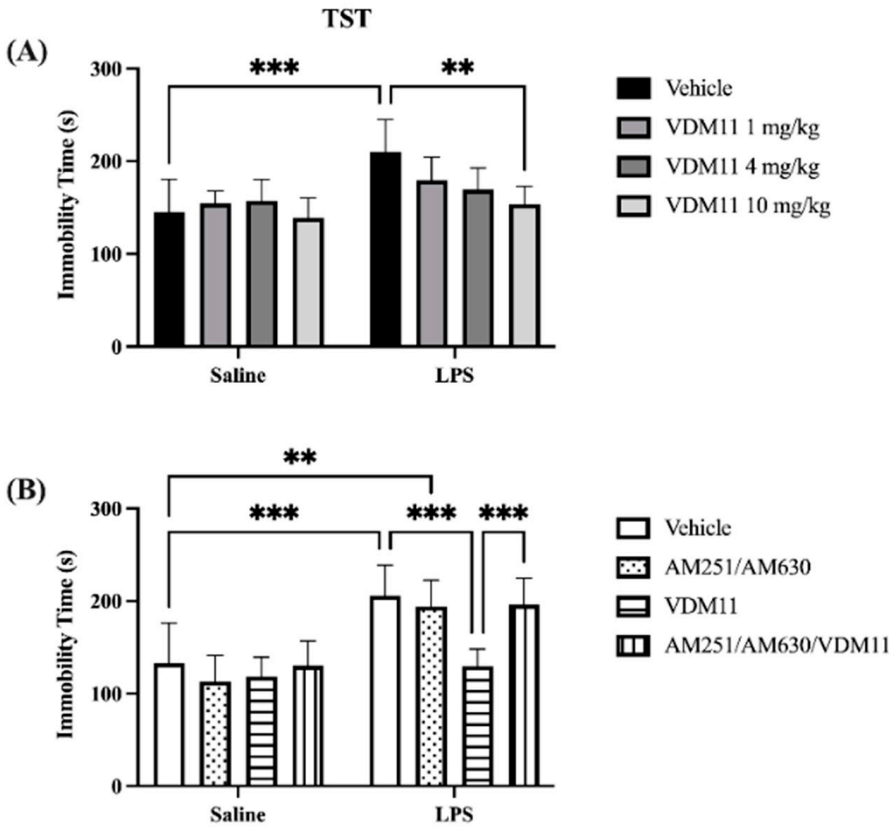

Figure 9. (**A**) A significant reduction in immobility time (s) during the tail suspension test (TST) 27 h after LPS treatment was achieved in mice when VDM11 (an anandamide reuptake inhibitor; 10 mg/kg) was used. (**B**) Combining treatment with 1 mg/kg of AM251 (a CB1 receptor antagonist) and 1 mg/kg of AM630 (a CB2 receptor antagonist) prevented the effects of 10 mg/kg of VDM11 on the decrease in immobility time (s) during the tail suspension test (TST) in mice 27 h after LPS administration. ** $p < 0.01$; *** $p < 0.001$.

3.3.5. Appraisal of VDM 11 Effect on Glial Cell Marker (CD11b and GFAP) in Hippocampus

The RT-PCR results depicted significant up regulation of mRNA expression of CD11b and GFAP in LPS-treated animals. However, no significant alterations were found in drug control groups which were treated with vehicle + saline and different doses of VDM11. Treatment of animals prophylactically with VDM11 and then exposure to LPS significantly down regulated the mRNA expressions of CD11b and GFAP at different doses. The most significant inhibition was achieved at 10 mg/kg of VDM11 (Figure 10A,C). Administration of CB1 antagonist (AM251) and CB-2 receptor antagonist (AM630) attenuated the VDM 11 influences on LPS-treated mice (Figure 10B,D).

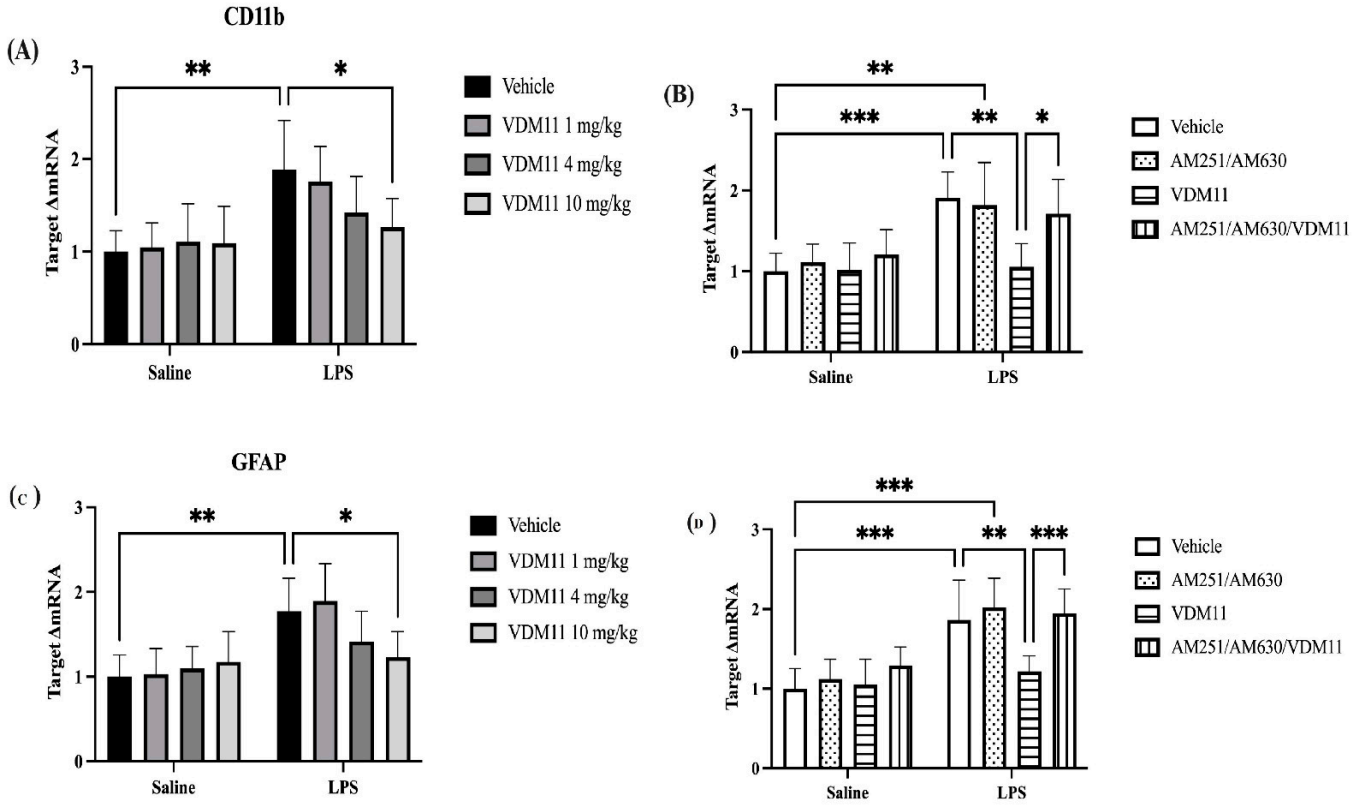

Figure 10. (**A**,**C**) anandamide reuptake inhibitor VDM11, 10 mg/kg, substantially reduced the LPS-induced elevation of CD11b and GFAP in the hippocampus. (**B**,**D**) Combining treatment with 1 mg/kg each of AM251 (a CB1 receptor antagonist) and AM630 (a CB2 receptor antagonist) mitigated the effects of 10 mg/kg of VDM11 on the elevation of CD11b and GFAP brought on by LPS injection in the hippocampus. * $p < 0.05$; ** $p < 0.01$; *** $p < 0.001$.

3.3.6. Assessment of VDM11 Effect on Proinflammatory Mediators (TNF-α, IL-1β, and IL-6) in Hippocampus

The results of RT-PCR assays conducted to estimate the proinflammatory cytokines in tissue homogenates (hippocampus) clearly demonstrated the significant increase in TNF-α, IL-1β, and IL-6 levels in normal animals when exposed to LPS. As noted in our previous findings, there were no significant alterations found in drug control animals in the levels of abovementioned proinflammatory cytokines when treated with vehicle + saline only and with different doses of VDM11. Pretreatment with VDM11 significantly lowered the generation of TNF-α, IL-1β, and IL-6 in animals exposed to LPS after 30 min of VDM11 treatment (Figure 11A–C). Antagonism of anandamide receptors CB1 and CB2 by AM251 and AM630, respectively, inhibited the prophylactic effects of VDM11 (Figure 12A–C). The most significant actions of VDM 11 were observed at 10 mg/kg.

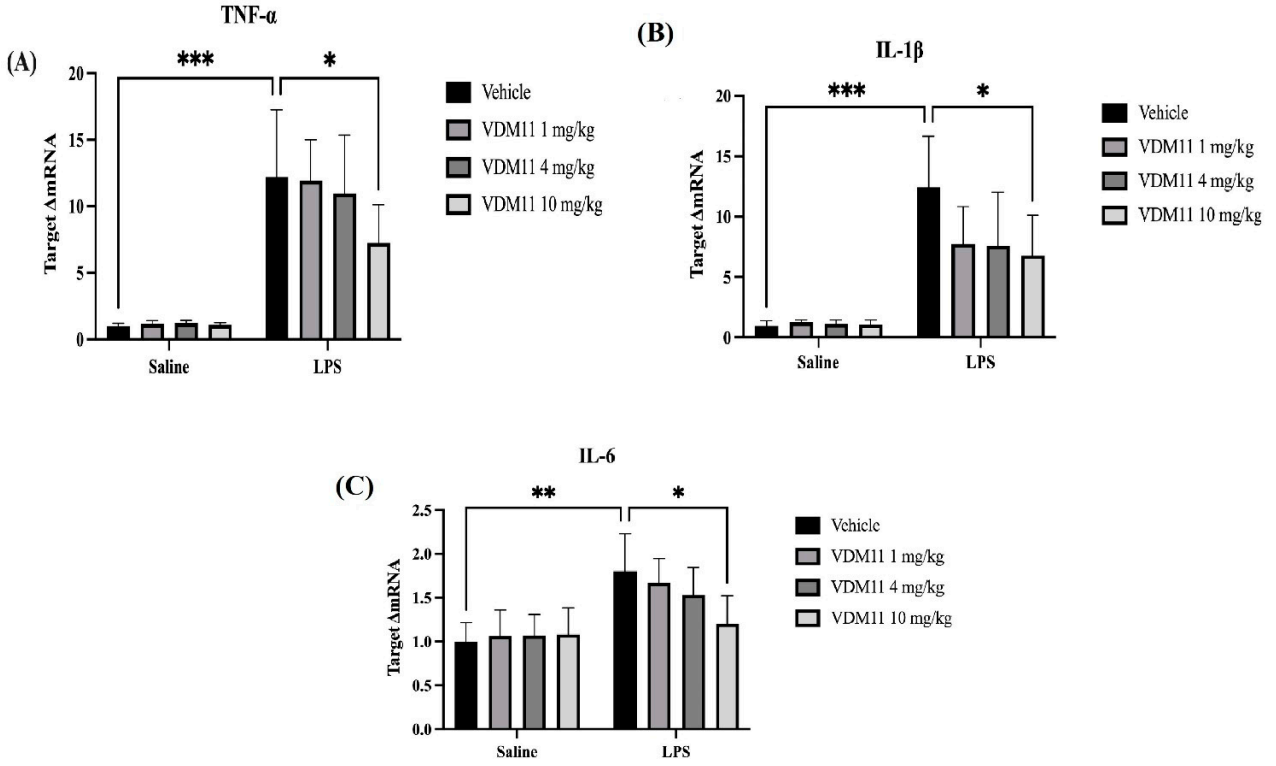

Figure 11. Anandamide reuptake inhibitor VDM11, 10 mg/kg, substantially lower LPS-induced elevation of TNF-α (**A**), IL1 (**B**), and IL6 (**C**) in the hippocampus. * $p < 0.05$; ** $p < 0.01$; *** $p < 0.001$.

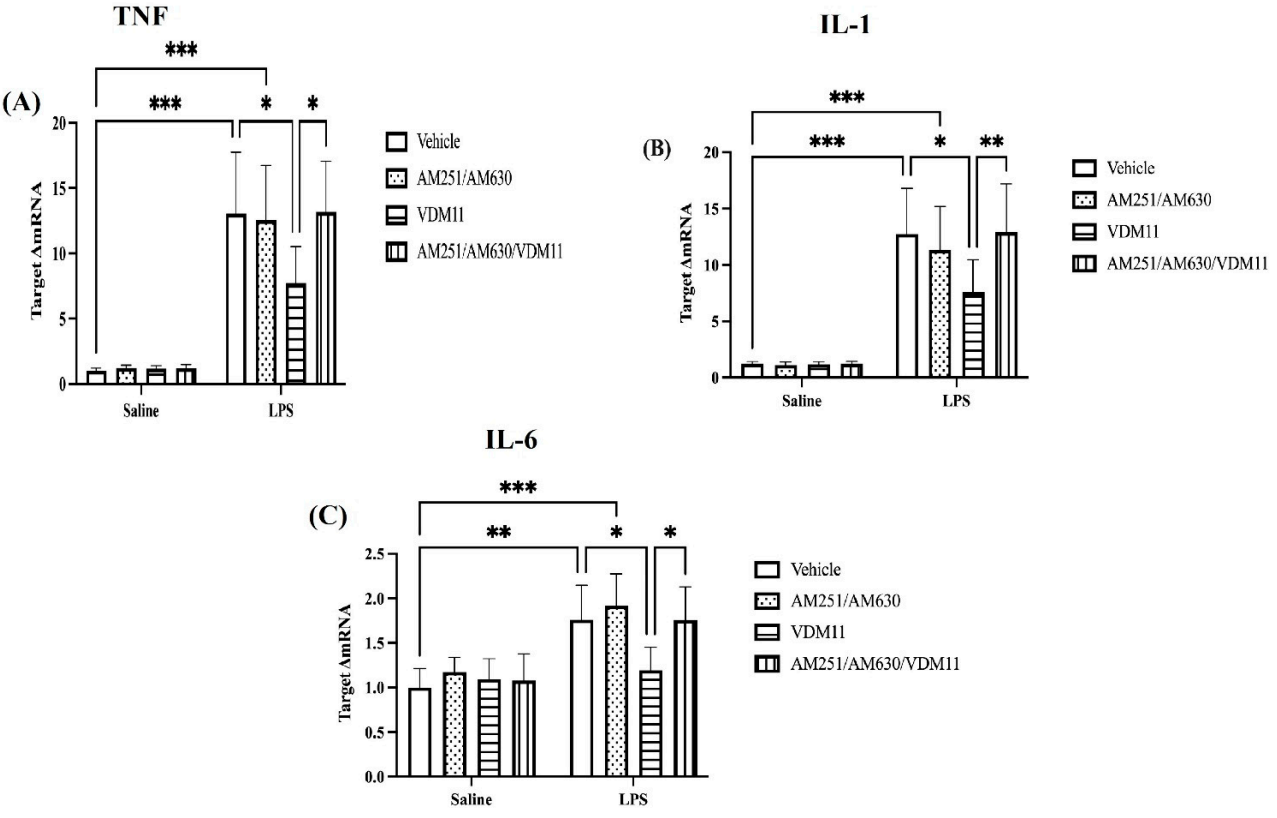

Figure 12. A combination treatment of 1 mg/kg each of AM251 and AM630 hindered the effects of 10 mg/kg of VDM11 on reducing the rise of TNF-α (**A**), IL1β (**B**), and IL6 (**C**) caused by LPS injection in the hippocampus.* $p < 0.05$; ** $p < 0.01$; *** $p < 0.001$.

4. Discussion

Psychopathological consequences during acute infection and in the post-infection phase in COVID-19 victims have been documented since the pandemic's emergence. Acute viral infection has been associated with delirium, sadness, anxiety, and sleep problems [2]. The immunological inflammatory response to the viral infection and probable resulting neuroinflammation, as well as the psychological stressors brought on by infection with SARSCoV-2, are the key factors contributing to the COVID-19 mental sequelae [27]. Given this context, it is necessary to describe, identify, and manage post-COVID-19 depression symptoms. As a result, in the proposed investigation, we aimed to anticipate VDM11's probable antidepressant effects on COVID-19 post-depression by employing network pharmacology, molecular docking, and an experimental pharmacology approach.

Since anandamide has a known role in reducing neuroinflammation [28], anandamide reuptake inhibitor VDM11 was our main focus, as neuroinflammation was proposed to be the major factor responsible for post-COVID depression. It has been suggested that microglial cells, which act as the CNS's resident phagocytes of the innate immune system, are the primary producers of anandamide [29]. Mood disorders have frequently been linked to immunologic dysregulation involving inflammatory processes. In fact, it is thought that one of the primary pathophysiological causes of major depressive disorder is the activation of innate immunity and the ensuing inflammation. It has been postulated that during COVID-19 infection, peripheral inflammatory signals, including TNF-α, IL-1β, and IL-6, increase the permeability of the blood–brain barrier (BBB). The compromised BBB may, in turn, make it easier for virus and other inflammatory mediators to enter the brain. Once inside the brain, cytokines can alter brain neurocircuits and neurogenesis, impairing some limbic system regions' functionality and resulting in depressive symptoms [30]. The activity of microglia and astrocytes can also be altered by inflammatory markers. Pro-inflammatory cytokines such as TNF-α, IL-1, IL-6, IL-12, and IL-23 are now released by activated microglia, and reactive oxygen (ROS) and reactive nitrogen species production is also increased. [30]. During depressive episodes, higher levels of IL-6 and TNF-α have been found to be associated with enhanced microglial activation [31], whereas microglia activation has been linked to both acute and long-term neurological consequences of COVID-19. Therefore, microglial-induced neuroinflammation appeared to be a promising target for managing post-COVID19 depression. Our research using molecular docking, network pharmacology, and experimental pharmacology showed that VDM 11 can change neuroinflammation in depression, most likely via changing TNF-α, IL-6, and IL-1β levels which is in accordance with previous studies.

A network pharmacology approach was used in the current investigation to postulate a possible mechanism of action of VDM11. PPI network analysis was performed to screen out the hub target genes of VDM11. Hub genes were screened on the basis of degree value so genes which have a higher degree value were selected [19]. The highest degree means that targeted genes are greatly correlated with each other; hence, all these genes might be key targets. The core genes were found to be MAPK3, TNF-α, IL-1β, IL-6, PPARG, MAPK1, CNR1, MTOR, NR3C1, and IGF1R. The function of each of these genes is discussed in Supplementary Table S1. GO and KEGG analysis revealed that these genes were enriched in the majority of functional annotations and biological pathways. According to GO functional analysis, antidepressant targets of VDM11 were mainly involved in regulation of acute inflammatory response, regulation of reactive oxygen species, and sensory perception of pain. KEGG pathway studies showed that target genes were involved mainly in neuroactive ligand–receptor interaction, HIF-1 signaling pathway, Th17 cell differentiation, and serotonergic synapse. Neuroactive ligand–receptor interaction signaling pathway relies mainly on neurotransmitter receptors which play a contributory role in a variety of psychological manifestations, including depression [17]. HIF-1 signaling pathway has an evident role in depression [32]. HIF-1 (Hypoxia-inducible factor) has gained attention as a potential target for depression therapy. Augmented HIF-1 levels have documented antidepressant attributes [33]. The serotoninergic synaptic pathway is made

up of serotonin and other serotonin receptors on synaptic membranes in various parts of the brain. Presynaptic membrane receptor hypersensitivity and postsynaptic membrane 5-HTIA receptor hypersensitivity have been found to be the main causes of depression Additionally, they may influence the release of other neurotransmitters such as dopamine (DA) and γ-amino butyric acid (GABA) [34]. After screening hub genes, the top five genes were selected for molecular docking analysis, which further confirms that VDM11 has strong binding interaction and high binding energy with selected target genes (MAPK3, TNF, IL1B, IL6, and PPARG).

In vivo studies employing the LPS-induced depression model confirmed the antidepressant attribute of VDM11 by using different tests. LPS has been documented to cause depression, mood changes, cognitive impairments, disturbed social activity, fatigue, and suppressed psychomotor behavior in experimental animals [35]. Our finding using OFT, the elevated plus maze test, Y maze test, and tail suspension test revealed the antidepressant effect of VDM11, which acts as an anandamide reuptake inhibitor acting primarily on C1 and C2 receptors. To confirm the hypothesis that VDM11 acts by enhancing anandamide binding with C1 and C2, antagonists for both C1 and C2 receptors (AM251 and AM 630) were administered to experimental animals prior to VDM11 administration. Blockage of receptors by administered antagonists diminished the antidepressant effect of VDM11, which confirmed the effect of VDM11 on cannabinoid receptors. LPS administration induces neuroinflammation in experimental animals by binding to TLR-4 receptors on microglia. Binding of LPS and activation of microglial cells further generates and releases proinflammatory mediators that contribute to depression. The microglial activation marker is CD11b and the biomarker for astrocyte activation is GFAP [36]. VDM11 administration leads to reduced mRNA expression of CD11b and GFAP, even after LPS administration confirmed the neuroinflammatory role of VDM11. Microglial cells activation after LPS administration resulted in release of proinflammatory mediators, including TNF-α, IL6, IL1β, prostanoids, and reactive oxygen species. Prophylactic treatment with VDM11 resulted in marked reduction in the levels of TNF-α, IL6, and IL1β which confirms that VDM11 not only prevents microglial cells activation but also can suppress the level of released proinflammatory mediators if microglial cells are activated by some means.

5. Conclusions

Based on the outcomes of the current study, which includes network pharmacology, molecular docking, and in vivo experimental analysis, it can be delineated that VDM11 might have the ability to suppress neuroinflammation, which has been described as a key mechanism responsible for post-COVID depression. Therefore, VDM11 can be considered a suitable candidate for COVID-19-associated depression. However, detailed pharmacological investigations are still required to point out the exact mechanism that might be responsible for the predicted antidepressant potential of VDM11.

Supplementary Materials: The following supporting information can be downloaded at: https://www.mdpi.com/article/10.3390/pr11010143/s1, Figure S1: Molecular docking of VDM11 and positive controls with selected targets; Table S1: Name of overlapping genes with their possible functions.

Author Contributions: Conceptualization, S.I.A. and S.Q.; methodology, S.Q.; software, M.A. (Muhammad Afzal); validation, S.I.A. and F.S.A.; formal analysis M.A. (Mohammed Alqinyah); investigation, S.I.A.; resources, M.A. (Metab Alharbi); data curation, H.H.A.; writing—original draft preparation, S.I.A.; writing—review and editing, S.Q. and O.A.A.; visualization, O.A.A.; supervision, S.I.A.; project administration, S.I.A.; funding acquisition, S.I.A. All authors have read and agreed to the published version of the manuscript.

Funding: This research was funded by Deanship of Scientific Research at Jouf University, grant number (CV-09-41).

Institutional Review Board Statement: Local Committee of Bioethics at Jouf University, Sakaka, Aljouf, Saudi Arabia (6-02-42) approved the Experimental protocol. All the experimental procedures

were carried out at the Pharmacology laboratory of College of Pharmacy, Jouf University, Sakaka, Al-Jouf, Saudi Arabia.

Informed Consent Statement: Not applicable.

Data Availability Statement: Not applicable.

Acknowledgments: The authors extend their appreciation to the Deanship of Scientific Research at Jouf University for funding this work through research grant No. (CV-09-41).

Conflicts of Interest: The authors declare no conflict of interest.

References

1. Kumar, A.; Singh, R.; Kaur, J.; Pandey, S.; Sharma, V.; Thakur, L.; Sati, S.; Mani, S.; Asthana, S.; Sharma, T.K.; et al. Wuhan to world: The COVID-19 pandemic. *Front. Cell. Infect. Microbiol.* **2021**, *30*, 242. [CrossRef] [PubMed]
2. Mazza, M.G.; Palladini, M.; Poletti, S.; Benedetti, F. Post-COVID-19 Depressive Symptoms: Epidemiology, Pathophysiology, and Pharmacological Treatment. *CNS Drugs* **2022**, *36*, 681–702. [CrossRef] [PubMed]
3. Vidrio, A.L.; Nicolini, H.; Zarate, C.T.; Castro, T.G.; Rojop, I.J.; Magaña, J.M.; López, N.M.; Mendoza, A.D.G. Association between SARS-CoV-2 Infection and Neuropsychiatric Manifestations. *COVID* **2022**, *2*, 1270–1286. [CrossRef]
4. Almutairi, M.M.; Sivandzade, F.; Albekairi, T.H.; Alqahtani, F.; Cucullo, L. Neuroinflammation and Its Impact on the Pathogenesis of COVID-19. *Front. Med.* **2021**, *8*, 745789. [CrossRef] [PubMed]
5. Zabetakis, I.; Lordan, R.; Norton, C.; Tsoupras, A. COVID-19: The Inflammation Link and the Role of Nutrition in Potential Mitigation. *Nutrients* **2020**, *12*, 1466. [CrossRef]
6. Sivandzade, F.; Alqahtani, F.; Sifat, A.; Cucullo, L. The cerebrovascular and neurological impact of chronic smoking on post-traumatic brain injury out-come and recovery: An in vivo study. *J. Neuroinflamm.* **2020**, *17*, 133. [CrossRef]
7. Matschke, J.; Lütgehetmann, M.; Hagel, C.; Sperhake, J.P.; Schröder, A.S.; Edler, C.; Mushumba, H.; Fitzek, A.; Allweiss, L.; Dandri, M.; et al. Neuropathology of patients with COVID-19 in Germany: A post-mortem case series. *Lancet Neurol.* **2020**, *19*, 919–929. [CrossRef]
8. Liu, L.-R.; Liu, J.-C.; Bao, J.-S.; Bai, Q.-Q.; Wang, G. Interaction of Microglia and Astrocytes in the Neurovascular Unit. *Front. Immunol.* **2020**, *11*, 1024. [CrossRef]
9. Zou, S.; Kumar, U. Cannabinoid Receptors and the Endocannabinoid System: Signaling and Function in the Central Nervous System. *Int. J. Mol. Sci.* **2018**, *19*, 833. [CrossRef]
10. Lu, H.-C.; Mackie, K. Review of the endocannabinoid system. *Biol. Psychiatry Cogn. Neurosci. Neuroim-Aging* **2021**, *6*, 607–615. [CrossRef]
11. Reggio, P.H. Endocannabinoid Binding to the Cannabinoid Receptors: What Is Known and What Remains Unknown. *Curr. Med. Chem.* **2010**, *17*, 1468–1486. [CrossRef]
12. Patel, S.; Hillard, C.J. Role of endocannabinoid signaling in anxiety and depression. In *Behavioral Neurobiology of the Endocannabinoid System*; Springer: Berlin/Heidelberg, Germany, 2009; pp. 347–371.
13. Gamaleddin, I.; Guranda, M.; Goldberg, S.R.; Le Foll, B. The selective anandamide transport inhibitor VDM11 attenuates reinstatement of nicotine seeking behaviour, but does not affect nicotine intake. *Br. J. Pharmacol.* **2011**, *164*, 1652–1660. [CrossRef]
14. Alzarea, S.I.; Qasim, S.; Uttra, A.M.; Khan, Y.H.; Aljoufi, F.A.; Ahmed, S.R.; Alanazi, M.; Malhi, T.H. Network Pharmacology and Molecular Docking Based Prediction of Mechanism of Pharmacological Attributes of Glutinol. *Processes* **2022**, *10*, 1492. [CrossRef]
15. Wang, X.; Yang, H.; Zhang, L.; Han, L.; Di, S.; Wei, X.; Wu, H.; Zhang, H.; Zhao, L.; Tong, X. Network Pharmacology-Based Prediction of Mechanism of Shenzhuo Formula for Application to DKD. *Evid. Based Complement. Altern. Med.* **2021**, *2021*, 6623010. [CrossRef]
16. Wang, W.; Liu, T.; Yang, L.; Ma, Y.; Dou, F.; Shi, L.; Wen, A.; Ding, Y. Study on the multi-targets mechanism of triphala on cardio-cerebral vascular diseases based on network pharmacology. *Biomed. Pharmacother.* **2019**, *116*, 108994. [CrossRef]
17. Nguyen, L.T.H.; Nguyen, N.P.K.; Tran, K.N.; Shin, H.-M.; Yang, I.-J. Network Pharmacology and Experimental Validation to Investigate the Antidepressant Potential of *Atractylodes lancea* (Thunb.) DC. *Life* **2022**, *12*, 1925. [CrossRef]
18. Cozza, G.; Moro, S. Medicinal Chemistry and the Molecular Operating Environment (MOE): Application of QSAR and Molecular Docking to Drug Discovery. *Curr. Top. Med. Chem.* **2008**, *8*, 1555–1572. [CrossRef]
19. Noor, F.; Rehman, A.; Ashfaq, U.A.; Saleem, M.H.; Okla, M.K.; Al-Hashimi, A.; AbdElgawad, H.; Aslam, S. Integrating Network Pharmacology and Molecular Docking Approaches to Decipher the Multi-Target Pharmacological Mechanism of *Abrus precatorius* L. Acting on Diabetes. *Pharmaceuticals* **2022**, *15*, 414. [CrossRef]
20. Landman, E.; Miclea, R.L.; van Blitterswijk, C.A.; Karperien, M. Small molecule inhibitors of WNT/β-catenin signaling block IL-1β-and TNFα-induced cartilage degra-dation. *Arthritis Res. Ther.* **2013**, *15*, R93. [CrossRef]
21. Brábek, J.; Jakubek, M.; Vellieux, F.; Novotný, J.; Kolář, M.; Lacina, L.; Szabo, P.; Strnadová, K.; Rösel, D.; Dvořánková, B.; et al. Interleukin-6: Molecule in the Intersection of Cancer, Ageing and COVID-19. *Int. J. Mol. Sci.* **2020**, *21*, 7937. [CrossRef]
22. Jarrar, M.H.; Baranova, A. PPARγ activation by thiazolidinediones (TZDs) may modulate breast carcinoma outcome: The importance of interplay with TGFβ signalling. *J. Cell. Mol. Med.* **2007**, *11*, 71–87. [CrossRef] [PubMed]

23. O'Connor, J.C.; A Lawson, M.; André, C.; Moreau, M.; Lestage, J.; Castanon, N.; Kelley, K.W.; Dantzer, R. Lipopolysaccharide-induced depressive-like behavior is mediated by indoleamine 2,3-dioxygenase activation in mice. *Mol. Psychiatry* **2009**, *14*, 511–522. [CrossRef] [PubMed]
24. Seibenhener, M.L.; Wooten, M.C. Use of the open field maze to measure locomotor and anxiety-like behavior in mice. *J. Vis. Exp.* **2015**, *96*, e52434. [CrossRef] [PubMed]
25. Tucker, L.B.; McCabe, J.T. Behavior of Male and Female C57BL/6J Mice Is More Consistent with Repeated Trials in the Elevated Zero Maze than in the Elevated Plus Maze. *Front. Behav. Neurosci.* **2017**, *11*, 13. [CrossRef] [PubMed]
26. Prieur, E.; Jadavji, N. Assessing Spatial Working Memory Using the Spontaneous Alternation Y-maze Test in Aged Male Mice. *Bio-Protocol* **2019**, *9*, e3162. [CrossRef]
27. Dehghani, A.; Zokaei, E.; Kahani, S.M.; Alavinejad, E.; Dehghani, M.; Meftahi, G.H.; Afarinesh, M.R. The potential impact of COVID-19 on CNS and psychiatric sequels. *Asian J. Psychiatry* **2022**, *72*, 103097. [CrossRef]
28. Walter, L.; Stella, N. Cannabinoids and neuroinflammation. *Br. J. Pharmacol.* **2004**, *141*, 775–785. [CrossRef]
29. Malek, N.; Popiolek-Barczyk, K.; Mika, J.; Przewlocka, B.; Starowicz, K. Anandamide, Acting via *CB2* Receptors, Alleviates LPS-Induced Neuroinflammation in Rat Primary Microglial Cultures. *Neural Plast.* **2015**, *2015*, 130639. [CrossRef]
30. e Silva, N.M.L.; Barros-Aragão, F.G.; De Felice, F.G.; Ferreira, S.T. Inflammation at the crossroads of COVID-19, cognitive deficits and depression. *Neuropharmacology* **2022**, *209*, 109023. [CrossRef]
31. Ting, E.Y.-C.; Yang, A.C.; Tsai, S.-J. Role of Interleukin-6 in Depressive Disorder. *Int. J. Mol. Sci.* **2020**, *21*, 2194. [CrossRef]
32. Fan, X.-X.; Sun, W.-Y.; Li, Y.; Tang, Q.; Li, L.-N.; Yu, X.; Wang, S.-Y.; Fan, A.-R.; Xu, X.-Q.; Chang, H.-S. Honokiol improves depression-like behaviors in rats by HIF-1α- VEGF signaling pathway activation. *Front. Pharmacol.* **2022**, *13*, 968124. [CrossRef]
33. Kang, I.; Kondo, D.; Kim, J.; Lyoo, I.K.; Yurgelun-Todd, D.; Hwang, J.; Renshaw, P.F. Elevating the level of hypoxia inducible factor may be a new potential target for the treatment of depression. *Med. Hypotheses* **2020**, *146*, 110398. [CrossRef]
34. Köhler, S.; Cierpinsky, K.; Kronenberg, G.; Adli, M. The serotonergic system in the neurobiology of depression: Relevance for novel antidepressants. *J. Psychopharmacol.* **2016**, *30*, 13–22. [CrossRef]
35. Cordeiro, R.C.; Chaves Filho, A.J.M.; Gomes, N.S.; Tomaz, V.D.S.; Medeiros, C.D.; Queiroz, A.I.D.G.; Maes, M.; Macedo, D.S.; Carvalho, A.F. Leptin prevents lipopolysaccharide-induced depressive-like behaviors in mice: Involvement of dopa-mine receptors. *Front. Psychiatry* **2019**, *10*, 125. [CrossRef]
36. Norden, D.M.; Muccigrosso, M.M.; Godbout, J.P. Microglial priming and enhanced reactivity to secondary insult in aging, and traumatic CNS injury, and neurodegenerative disease. *Neuropharmacology* **2015**, *96*, 29–41. [CrossRef]

Disclaimer/Publisher's Note: The statements, opinions and data contained in all publications are solely those of the individual author(s) and contributor(s) and not of MDPI and/or the editor(s). MDPI and/or the editor(s) disclaim responsibility for any injury to people or property resulting from any ideas, methods, instructions or products referred to in the content.